Evaluation of the Unsaturated Shear Strength Parameters of Compacted, Heaving Soil Using Geotechnical Properties

Armand Augustin Fondjo[1*], *Elizabeth* Theron[2], and *Richard P* Ray[3]

[1 2]Department of Civil Engineering, Central University of Technology, 20 President Street, Bloemfontein, 9300, South Africa
[3]Structural and Geotechnical Engineering Department, Széchenyi István Egyetem University, 9026 Gyor, Egyetem tér 1, Hungary

Abstract The shear strength is a fundamental property of soil material under structural loads. The determination of shear strength properties of unsaturated soils is challenging and time-consuming. Geotechnical predictive models can be utilized to assess the unsaturated shear strength of heaving soil. This study attempts to propose predictive models to evaluate the unsaturated shear strength parameters of compacted heaving soil. These parameters include the angle of internal friction associated with the net normal stress (ϕ'), angle indicating the rate of increase in shear strength with respect to a change in matric suction (ϕ^b), and effective cohesion (c'). The geotechnical properties of soils were assessed through laboratory tests such as particle size distribution, consistency limits, specific gravity, modified Proctor compaction test, swelling test, suction test, and advanced triaxial testing. Multivariate analysis was conducted using NCSS 12 software to design the models. The validation of models includes the determination coefficient, probability value, comparing experimental values with predicted values, and comparing the developed models with other model found in recent literature. The models engineered in this study can estimate the unsaturated shear strength parameters of compacted heaving soil with acceptable precision.

1 Introduction

The shear strength is a fundamental property that governs the stability of soil material under structural loads. Then, it is required to determine the shear strength parameters and stiffness of soil support in foundation design. The bearing limit, slope stability, lateral earth pressures, etc., are some examples of geotechnical application related to the shear strength. Terzaghi [1] used the effective stress variable and Mohr-Coulomb failure criterion to formulate a mathematical relation to predict the shear strength of saturated soils described in Equation (1). τ_s is the saturated shear strength, ($\sigma_n - u_w$) the effective normal stress, c' the cohesion, and ϕ' angle of internal friction.

$$\tau_s = c' + (\sigma_n - u_w)\, tan\, (\phi') \quad (1)$$

The foundation of structures is generally located above groundwater table and is in unsaturated conditions. Unsaturated soils behaviour has received attention from researchers whose common objective has been to develop an appropriate expression that adequately models the shear strength of soil material. The principle of shear strength of unsaturated soils is described as an extension of mathematical equation of shear strength for saturated soils describes by Mohr-Coulomb failure criterion (Mohr [2]). The Mohr-Coulomb criterion extension is referred as the extended Mohr-Coulomb failure criterion for unsaturated soil. Moreover, the stress condition of partially saturated soils can be represented utilizing the suction matric ($u_a - u_w$) and net normal stress ($\sigma_n - u_a$). The contribution of matric suction is commonly added to the shear strength equation of saturated soil to describe the shear strength of unsaturated soils. Fredlund and Rahardjo [3] developed a shear strength constitutive relation for unsaturated soils given in Equation (2). τ_u is the unsaturated shear strength, ϕ^b the angle indicating the rate of increase in shear strength with respect to a change in matric suction ($u_a - u_w$).

$$\tau_u = c' + (\sigma_n - u_a)\, tan\, (\phi') + (u_a - u_w)\, tan\, (\phi^b) \quad (2)$$

Blight [4] reported challenges related to the shear strength measurement for unsaturated soils. The challenges include the need of several tests to establish the strength variation with matric suction. A long time is required to achieve the matric suction equilibrium in soil specimens before testing. Fondjo [5] reported that axis-translation technique applied effectively on modified-triaxial cell for shear strength testing of unsaturated soils exhibits a matric suction range of 0 to 1500 kPa. Rao and Revanasiddappa [6] mentioned that in compacted soil clay specimens, the matric suction ranges from 50 kPa to 8000 kPa at saturation values of 35% to 90%. In a similar study, Fondjo et al. [7] reported that compacted heaving soil exhibits a matric suction range of 40 kPa to 7700 kPa, and a total suction range of 55 kPa to 10 000 kPa. Models to predict the shear strength of saturated soils in Table 1 have been reported

* Corresponding author: fondjoarmand1976@gmail.com

in the literature (Chen et al [8]; Roy and Dass [9]). Nonetheless, little consideration was given to model to predict the unsaturated shear strength of compacted heaving soil. Thus, the development of a geotechnical predictive model for unsaturated shear strength characteristics is necessary to address the problem.

Table 1. Predictive equations

Reference	Equations
Chen et al. [8]	$\text{Log}(\phi') = -(0.0186W + 0.28)\gamma_d + 0.0141W - 1.15$ $c' = -4.13W + 149.4$
Roy and Dass [9]	$\phi' = -29.604 + 34.220\gamma_d$ $c' = -0.525 + 24.1G_S$

2 Methods

2.1 Laboratory testing

The evaluation of geotechnical properties of soil samples was performed following the standards: ASTM D4220-14[10] standard practices for preserving and transporting soil samples, SANS 3001-GR20 [11] moisture content determination, SANS 3001-GR2 [12] sieve analysis. SANS 3001-GR3 [13] sedimentation analysis. ASTM D854-14 [14] specific gravity test. SANS 3001-GR10 [15] consistency limits test. IS: 2720-part 40, 1977 [16] free swell index. Sridharan & Prakash [17] free swell ratio. SANS 3001-GR30 [18] Proctor compaction test. ASTM D5298-16 [19] soil suction measurement using filter paper technique. ASTM D4767- 99 [20] triaxial testing.

2.2 Sample preparation

A similar set of soil specimens were prepared for each sample at different moisture content throughout the compaction test. One set of soil specimens was used for soil suction test and another set was used for triaxial testing. An average of two results for each tested soil specimen was considered the most consistent results estimated in laboratory.

2.3 Geotechnical predictive model design

The modeling process conducted in this study is as follows: data collection, selection of covariates for each predictive model design, model specification, and model validation. The geotechnical models were designed using NCSS 12 Software. The model selection was conducted by testing different models, including logarithmic, quadratic, linear, cubic, power, and exponential. It was found that the linear model displays a higher strength correlation and best-fitting equation. Johnson [21] reported that the predictive multi-linear model takes the form of Equation 3.

$$Y = + \xi_o + [\sum \xi_i \times Z_i] + \varepsilon \quad (3)$$

Where:

Y= outcome variable
ξ_o= intercept
ξ_i= regression coefficients, i=1,2,3, …n
Z_i= covariates, i=1,2,3, …n
n= number of covariates
ε= random error term

The validation of models includes the determination coefficient, probability value, and comparing experimental value with predicted value.

3 Results and discussion

3.1 Material properties

The particle size analysis revealed that the fine-grained content is not uniform for studied soils. WES exhibits the highest amount of fine-grained among other soil samples, followed by WIS, BFS, and BES. More than 50% of these soils passed the No 200 (0.075mm) sieve. Nonetheless, BES show a fine-grained content of 45.14%. The tested soils have a liquid limit of 40.29% to 69.45% and a plastic limit of 19.23% to 49.23%. Soil samples are classified using Universal Soil Classification System. BFS, WIS, WES display a high plasticity, and BES displays a low plasticity. Table 2 shows the summary of soil material properties.

Table 2. Material properties

Soils	Liquid limit (%)	Plasticity index (%)	Clay (%)	Silt (%)	Sand (%)	Gravel (%)	Specific Gravity (Gs)	USCS
BFS	58.98	36.82	30.40	29.11	29.39	10.09	2.64	CH
WIS	63.78	42.48	34.03	33.49	26.80	4.85	2.73	CH
WES	69.45	49.87	40.00	33.00	23.50	2.56	2.73	CH
BES	40.29	19.23	17.11	28.03	43.76	11.10	2.55	CL

3.2 Swelling potential analysis

The tested soils exhibit a swelling behaviour with a free swell index range of 35.81 % to 116.60 %, and a free swell ratio range of 1.17 to 2.20. Table 3 shows the swelling potential test results.

Table 3. Swelling potential test results

Soil	Swelling potential Classification IS 2720 - 40 [16]		Swelling potential classification, Sridharan & Prakash [17]	
	Free swell index (FSI)	Soil expansivity	Free swell ratio (FSR)	Soil expansivity
BFS	64.31	Moderate	1.64	Moderate
WIS	81.37	Moderate	1.73	Moderate
WES	116.60	High	2.20	High
BES	35.81	Moderate	1.17	Low

3.3 Suction test results

The total suction consists of two primary components, the matric suction and osmotic suction. The matric suction is a fundamental parameter controlling the behaviour of unsaturated soils. The reported suction values were measured at a different moisture content at the initial state utilizing the Whatman No 42 type filter paper technique (FPT). The principle of FPT is to measure the suction indirectly by relating the water absorbed by specified filter paper with suction through

a calibration curve. Table 4 in Appendix shows the suction test results. The tested soils have a total suction of 110 kPa to 9926 kPa, a matric suction of 80 kPa to 7694 kPa, and an osmotic suction of 30 kPa to 2232 kPa.

3.4 Triaxial testing results

The consolidated undrained triaxial tests were conducted on prepared unsaturated soil specimens at each water content. The shear strength characteristics were recorded automatically by INSTRON triaxial software. The Mohr - Coulomb shear strength criterion extension to unsaturated soils requires the evaluation of saturated shear strength characteristics (c', ϕ'). The angle ϕ^b related to the matric suction are measured as the slope between the shear strength and matric suction curve denoted unsaturated soil failure envelope. The unsaturated failure envelope for sample WIS with ϕ^b = 5.02° is shown in Figure 1. Moreover, the reported values of ϕ^b for BFS, WES, and BES are 6.77°, 2.67° and 10° respectively. The triaxial test results is shown in Table 5 Appendix. The reported unsaturated shear strength (τ_u) values range from 196 kPa to 1512 kPa, and the saturated shear strength (τ_s) values range from 154 kPa to 941 kPa. τ_u values are 1.1 to 1.78 times higher than (τ_s) values due to the contribution of matric suction. The studied soils have a friction angle (ϕ') of 25º to 53º, an angle related to matric suction (ϕ^b) of 2.67º to 10º, and cohesion (c') of 45 kPa to 78 kPa. The results of ϕ' and ϕ^b concord with the research works published by Fredlund and Rahardjo [3], Likos et al. [22], and Nam et al. [23] reported that ϕ^b is smaller than ϕ', ($\phi^b < \phi'$).

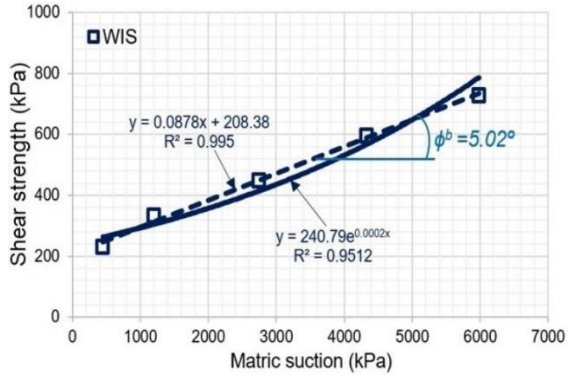

Fig. 1. Unsaturated failure envelope for WIS

4 Models development

The unsaturated shear strength parameters (ϕ', ϕ^b, c') were investigated in relation to geotechnical index properties to select the covariates for each model. Regression analysis is performed through NCSS 12 Software based on correlation matrices given in Tables 2, 4 and 5 to design the models for angle of internal friction (ϕ'), angle indicating the rate of increase in shear strength with respect to a change in matric suction (ϕ^b), and effective cohesion (c'). The probability value was used to select the covariate. When p-value of covariate coefficient is higher than 0.05, the coefficient is considered 0, the covariate is viewed as insignificant and excluded from the model. Table 6 shows the summary of p-values of unsaturated shear strength parameters (ϕ', ϕ^b, c').

Table 6. P-value of unsaturated shear strength parameters

Saturated friction Angle, ϕ' (º)		Matric suction angle, ϕ^b (º)		Cohesion, c' (kPa)	
Term	p-value	Term	p-value	Term	p-value
W (%)	0.000	G_s	0.002	LL (%)	0.031
γ_d (k.N.m^{-3})	0.045	Void ratio (e)	0.054	Clay (%)	0.018
FSI (%)	0.063	W (%)	0.000	Fine (%)	0.046
FSR	0.071	γ_d (k.N.m^{-3})	0.038	Void ratio (e)	0.051
Clay (%)	0.012	FSR	0.055	C_u	0.060
Fine (%)	0.022	FSI (%)	0.063	FSI (%)	0.060
G_s	0.003	C_u	0.058	FSR	0.081
Void ratio (e)	0.058	PI (%)	0.025	G_s	0.006
LL (%)	0.011	LL (%)	0.018	γ_d (k.N.m^{-3})	0.004
PI (%)	0.015	Clay (%)	0.038	W (%)	0.031
C_u	0.061	Fine (%)	0.027	PI (%)	0.000

4.1 Estimated models

Equation 4 describes the predictive model for the angle of internal friction (ϕ'). Equation 5 describes the predictive model for the angle indicating the rate of increase of shear strength for a change in matric suction (ϕ^b). Equation 6 describes effective cohesion (c'). Table 7 in Appendix shows the developed models' summary and coefficients.

4.1.1 Predictive model (ϕ')

$$(\phi')^{\lambda} = -\xi_o - \xi_1 W + \xi_2 G_s + \xi_3 PI - \xi_4 LL - \xi_5 Clay - \xi_6 Fine \quad (4)$$

Where:

ϕ' (°)= angle of internal friction associated with the net normal stress
W (%) = gravimetric water content
G_s = specific gravity
PI (%) = plasticity index
LL (%) = liquid limit
Fine (%) = fine content
Clay (%) = clay content
λ = Box-cox transformation,
ξ_o = intercept
ξ_i = multivariate coefficients, i= 1, 2.…6.

4.1.2 Predictive model (ϕ^b)

$$(\phi^b)^{\lambda} = +\eta_o - \eta_1 W + \eta_2 G_s - \eta_3 Fine + \eta_4 LL - \eta_5 \gamma_d \quad (5)$$

Where:

ϕ^b (°)= angle indicating the rate of increase of shear strength for a change in matric suction
W (%) = gravimetric water content
G_s = specific gravity
LL (%) = liquid limit
Fine (%) = fine content
γ_d (kN.m^{-3}) = dry unit weight
λ= Box-cox transformation
η_o= intercept
η_i= multivariate coefficients, i= 1, 2,…5

4.1.3 Predictive model (c')

$$(c')^{\lambda} = -\zeta_o - \zeta_1 W - \zeta_2 Fine + \zeta_3 G_S - \zeta_4 LL + \zeta_5 PI \quad (6)$$

Where:

c' (kPa)=	effective cohesion
W (%) =	gravimetric water content
G_s =	specific gravity
PI (%) =	plasticity index
LL (%) =	liquid limit
Fine (%) =	fine content
λ=	Box-cox transformation,
ζ_o =	intercept
ζ_i =	multivariate coefficients, i= 1, 2,….5.

4.2 Models validation

4.2.1 Validation of predictive model (ϕ')

Figure 2 shows the graph data of measured friction angle and predicted friction angle values at different water content. The variation of measured friction angle is comparable to predicted friction angle values. The scattered plotted data exhibits marginal disparities, and the relation between measured and predicted values of friction angle describes a high strength correlation with a determination coefficient of 92.48 %. Furthermore, the present model is compared with model by Chen et al. [8] in Table 1. The model by Chen et al. [8] bears a good correlation (Figure 3). This model was developed on compacted heaving soil. The predicted values of model by Chen et al. [8] agreed with the model developed in this study. Nevertheless, the present model is more accurate and portrays a high-strength correlation. The precision of the model proposed in this study may come from the higher number of covariates. The model by Chen et al. [8] is designed using 1 to 2 covariates. Fondjo and Dzogbewu [24] mentioned that the marginal discrepancies between experimental values and predicted values may also be due to the inherent approximated approach in multivariate analysis.

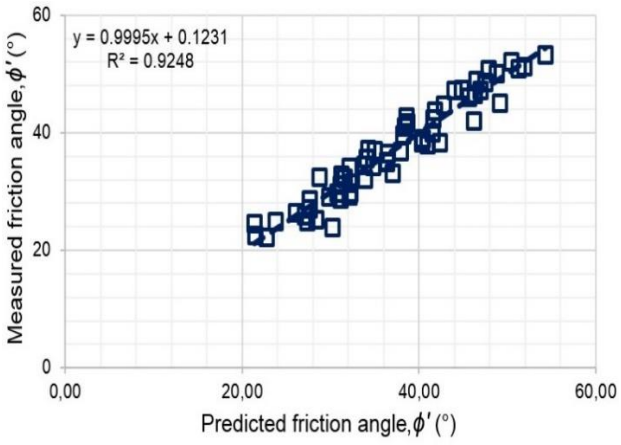

Fig. 2. Measured vs predicted values of (ϕ')

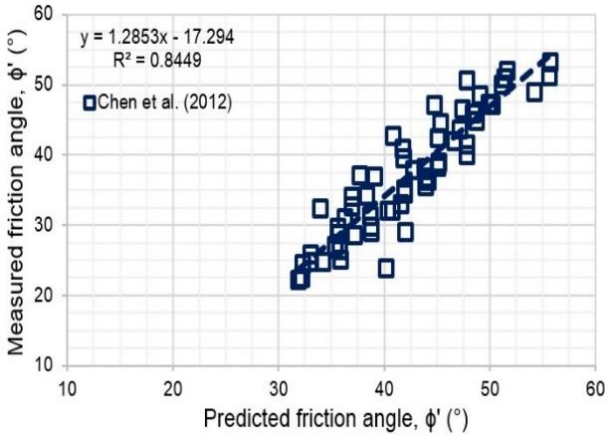

Fig. 3. Measured vs predicted values of (ϕ′)
Model Chen et al. [8]

4.2.2 Validation of predictive model (ϕ^b)

Figure 4 portrays the plotted data of measured angle indicating the rate of increase in shear strength with respect to change in matric suction (ϕ^b) versus the predicted values of ϕ^b obtained from the compacted soil specimens at different water content.

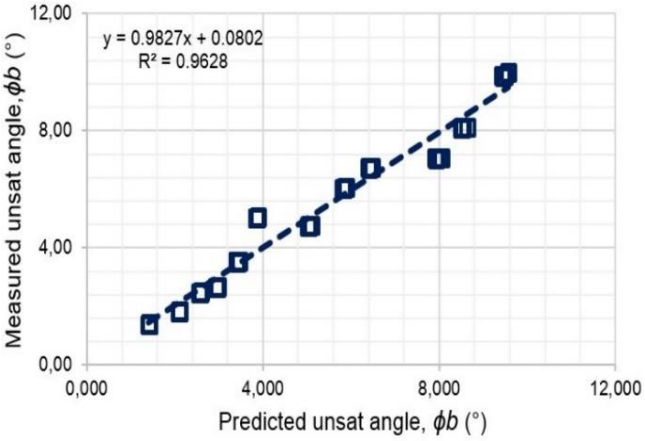

Fig. 4. Measured vs predicted values of (ϕ^b)

The graph data follows the trend line 1:1 and describes a high strength correlation between the measured values of ϕ^b and predicted values of ϕ^b with a determination coefficient of 96.28%.

4.2.3 Validation of predictive model (c')

Figure 5 shows the curve data of measured cohesion and predicted cohesion values of compacted specimens at different water content. The change in estimated cohesion is quite similar to predicted cohesion values. Besides, the plotted data displays marginal disparities. The relation between the predicted and measured cohesion values portrays a high-strength relationship with a determination coefficient of 94.41 %.

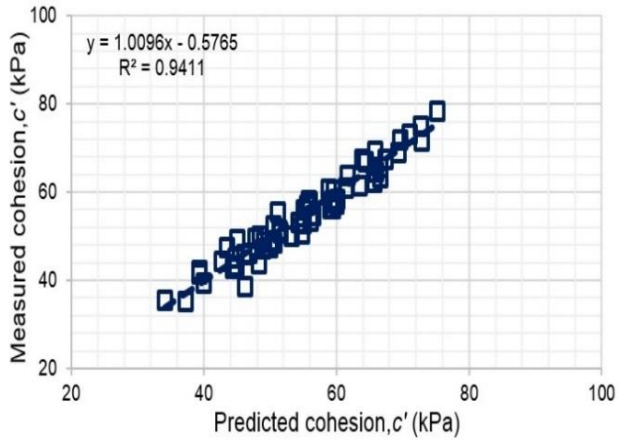

Fig.5. Measured vs predicted values of (c′)

Furthermore, the model developed in this study is compared to the model proposed by Chen et al. [8] in Table 1. Figure 6 shows the plotted data of the measured and predicted cohesion obtained through different model. The model by Chen et al. [8] portrays a good correlation. The model by Chen et al. [8] is developed using compacted heaving soil like the present model. The predicted values of the model proposed by Chen et al. [8] concurred with the model engineered in this study. The present model is more accurate and portrays a high strength correlation.

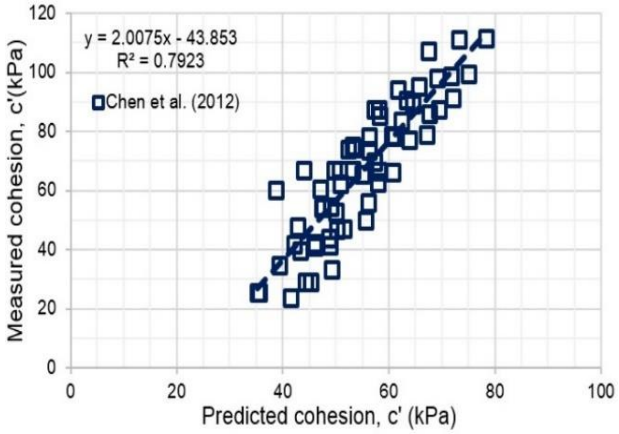

Fig. 6. Measured vs predicted values of (c′)
Model Chen et al. [8]

5 Conclusion

The research work clearly illustrates that the three geotechnical predictive models designed in this study are efficient tools to predict the unsaturated shear strength parameters of compacted heaving soil with acceptable precision, and reduce the cost and time required for laboratory testing. These parameters include the angle of internal friction associated with the net normal stress (ϕ'), angle indicating the rate of increase in shear strength with respect to a change in matric suction (ϕ^b), and effective cohesion (c').

In recognition of the support provided by the National Research Foundation (MND210624615504), the first author extend his sincerest gratitude.

Reference

1. K. Terzaghi, *The shear strength of saturated soils,* in Proceeding. 1st International Conference in Soil Mechanics and Foundation Engineering, Cambridge **1**, 54-56 (1936)
2. H. Mohr, Geologie der wechselbahn, insbesondere des grossen Hartbergtunnels (Vienna-Kais. Akad. d. Wissensch, 1914)
3. D.G. Fredlund, H. Rahardjo, Soil mechanics for unsaturated soils (John Wiley & Sons, 1993)
4. G.E. Blight, Unsaturated soil mechanics in geotechnical practice (CRC Press, 2013)
5. A.A. Fondjo, *Characterization of shear stress properties of compacted, unsaturated heaving soils*. D.Eng. Thesis, Central University of Technology, Free State. (to be published)
6. S.M. Rao, K. Revanasiddappa, J. of Geotech. and Geoenv. Eng **126**, 1 (2000)
7. A.A. Fondjo, E. Theron, R.P. Ray, *Models for predicting the suction of heaving compacted soils using geotechnical properties*, in Proceedings of the 14th Baltic Sea Geotechnical Conference, BSGC, 18-19 January 2021, Helsinki, Finlande (2021)
8. Y. Chen, J. Zhao, X.H. Hu, X.H, Appl. Mech. and Mat **256**, 287-292 (2012)
9. S. Roy, G. Dass, India. Inter. J. of Civ. and Stru. Eng **4**, 4 (2014)
10. ASTM D4220-14 ASTM International, www.astm.org (2014)
11. SANS 3001 Part GR20 SABS Standards Division, www.sabs.co.za (2010)
12. SANS 3001 Part GR2 SABS Standards Division, www.sabs.co.za (2011)
13. SANS 3001 Part GR3 SABS Standard Divisions, www.sabs.co.za (2012)
14. ASTM D854-14 ASTM International, www.astm.org (2014)
15. SANS 3001 Part GR10 SABS Standards Division, www.sabs.co.za (2011)
16. BIS IS 2720- Part 40 Bureau of Indian Standard, www.bis.gov.in (1977)
17. A. Sridharan, K. Prakash, *Classification procedures for expansive soils*, in Proceedings of the Institution of Civil Engineers-Geotechnical Engineering **143**, 4 (2000)
18. SANS 3001 Part GR30 SABS Standard Divisions, www.sabs.co.za (2015)
19. ASTM D5298-16 ASTM International, www.astm.org (2016)
20. ASTM D4767-99 ASTM International, www.astm.org (1999)
21. R.A. Johnson, Miller & Freund's probability and statistics for engineers (Ninth Edition, Pearson Education Limited, 2017)
22. W.J. Likos, A. Wayllace, J. Godt, N. Lu, Geotech. Test. J **33**, 4 (2010)
23. S. Nam, M. Gutierrez, P. Diplas, J. Petrie, Eng. Geol **122**, 272–280 (2011)
24. A.A. Fondjo, T.C. Dzogbewu, Univ. J. of Mech. Eng **7**, 6 (2019)

Appendix

Table 4. Suction test results

Soils	Soil water content (%)	Dry unit weight, (kN/m³)	Total suction (kPa)	Matric suction (kPa)	Osmotic suction (kPa)
BFS	12.06	15.60	5883.92	4741.62	1142.3
	14.02	16.21	4064.22	3327.18	737.04
	17.03	17.01	1923.09	1388.22	534.87
	20.07	17.58	1036.11	671.89	364.22
	24.8	17.20	340.034	200	140.034
WIS	14.98	15.60	7439.15	5984.56	1454.59
	17.50	16.05	5410.66	4332.678	1077.982
	21	16.58	3580.89	2748.30	832.59
	24.03	16.85	1699.05	1199.35	499.70
	28.06	16.70	816.77	450.227	366.543
WES	15.93	14.94	9926.183	7693.666	2232.517
	19.25	15.48	6922.321	5227.777	1694.544
	23.37	16.09	4011.482	2986.456	1025.026
	26.14	16.29	2475.62	1778.651	696.969
	29.10	15.85	1397.745	890.47	507.275
BES	9.18	16.35	4163.35	3312.26	851.09
	12.42	18.01	2510.04	1982.31	527.73
	14.54	18.95	830.926	538.11	292.816
	17.23	19.60	323.818	225.609	98.209
	20.30	19.10	109.66	79.70	29.96

Table 5. Unsaturated shear strength parameters

Soil	Moisture content (%)	c' (kPa)	tan (ϕ') (Degree)	(σ_n-u_a) (kPa)	τ_s (kPa)	(u_a-u_w) (kPa)	tan (ϕ^b) Degree	τ_u (kPa)
BFS	12.06	75.05	52.09	605.5	853	4741.62	6.77	1414.44
	14.02	72.05	48.55	547.78	692	3327.18	6.77	1086.56
	17.03	67.11	44.65	485.53	547	1388.22	6.77	711.25
	20.07	58.10	39.66	406.30	395	671.89	6.77	474.56
	24.80	51.54	32.71	333.87	266	200	6.77	289.67
WIS	14.98	69.42	50.75	537.59	727	5984.56	5.02	1253.44
	17.50	63.89	47.18	492.32	595	4332.68	5.02	976.02
	21	57.95	42.75	423.28	449	2748.30	5.02	690.80
	24.03	55.60	37.21	365.56	333	1199.35	5.02	438.60
	28.06	49.30	32.51	282.94	230	450.23	5.02	269.20
WES	15.93	62.39	42.07	452.71	471	7693.67	2.67	830.31
	19.25	57.32	37.95	413.10	379	5227.78	2.67	623.62
	23.37	50.11	34.31	328.78	274	2986.46	2.67	413.94
	26.14	48.85	28.8	284.07	205	1778.65	2.67	288.08
	29.1	45.31	24.92	234.84	154	890.47	2.67	196.01
BES	9.18	78.34	53.21	645.11	941	3312.26	10	1512.02
	12.42	69.05	50.08	554.57	732	1982.31	10	1073.58
	14.54	64.56	46.03	503.07	586	538.11	10	678.82
	17.23	61.09	42.42	431.77	456	225.61	10	494.52
	20.3	54.93	33.05	350.85	283	79.70	10	296.95

Table 7. Models summary and coefficients

Models	R^2	R^2 (adj)	R^2 (pred)	Intercepts	Coefficients
Saturated friction angle, ϕ' (°)	92.78	91.97	90.64	$\xi_o = 12.13$	$\xi_1 = 0.1397$; $\xi_2 = 11.2400$; $\xi_3 = 0.2208$; $\xi_4 = 0.0888$; $\xi_5 = 0.0296$; $\xi_6 = 0.1810$ Box-cox transformation, λ= 0.482967
Matric suction angle, ϕ^b (°)	96.64	96.33	96.05	$\eta_o = 5.68$	$\eta_1 = 0.00062$; $\eta_2 = 0.0300$; $\eta_3 = 0.0939$; $\eta_4 = 0.0424$; $\eta_5 = 0.0081$ Box-cox transformation λ= 0.5
Cohesion, C' (kPa)	93.76	93.18	92.21	$\zeta_o = 9.22$	$\zeta_1 = 0.1239$; $\zeta_2 = 0.2616$; $\zeta_3 = 11.390$; $\zeta_4 = 0.0848$; $\zeta_5 = 0.2641$ Box-cox transformation λ= 0.5